Breast Cancer Histopathological Image Classification using Progressive Resizing Approach

Hendra Bunyamin[1][a], Hapnes Toba[1][b], Meyliana[2][c] and Roro Wahyudianingsih[3][d]

[1]Informatics Engineering, Maranatha Christian University, Jl Prof. drg. Surya Sumantri, M.P.H. No. 65, Bandung, Indonesia
[2]Accounting Department, Maranatha Christian University, Jl Prof. drg. Surya Sumantri, M.P.H. No. 65, Bandung, Indonesia
[3]Faculty of Medicine, Maranatha Christian University, Jl Prof. drg. Surya Sumantri, M.P.H. No. 65, Bandung, Indonesia

Keywords: Breast Cancer Histopathological Image Classification, Deep Learning, Convolutional Neural Network, Progressive Resizing, Vahadane Image Normalization.

Abstract: Breast cancer (BC) is a lethal disease which causes the second largest number of deaths among women in the world. A diagnosis of biopsy tissue stained with hematoxylin & eosin, commonly named BC histopathological image, is a non-trivial task which requires a specialist to interpret. Recently, the advance in machine learning techniques driven by deep learning techniques and competition datasets has enabled the automation and prediction of histopathological images interpretation. Each different competition dataset has its own state-of-the-art technique; therefore, this paper explores an avenue of research by merging popular BC histopathological images research datasets and searching for the best performing models on the unified dataset. The merging process maintains similar classes among the datasets; consequently, the unified dataset has three classes and the prediction problem is cast into multi-class classification problem. We propose a combination of Vahadane preprocessing technique and training method using progressive resizing approach. Our approach demonstrates that both utilizing Vahadane image normalization and utilizing our progressive resizing technique achieve around 99% in F_1 score, which is comparable among other state-of-the-art models. The unified dataset is also provided online for advancing research in histopathological images interpretation.

1 INTRODUCTION

Breast cancer (BC) is the cause of the second largest deaths among women (Spanhol et al., 2016; Bray et al., 2018; McKinney et al., 2020) in the world. Data Global Cancer Observatory 2018 from World Health Organization (WHO) showed that the most number of cancer cases in Indonesia is BC with 58,256 of 348,809 patients or 16.7% (World Health Organization, 2018). However, cancer screening research encompassing imaging procedures, such as diagnostic mammogram (X-rays), magnetic resonance imaging, ultrasound (sonography), and thermography has been conducted for more than four decades and deemed beneficial to likely lessen number of deaths caused by BC significantly (Stenkvist et al., 1978; Institute of Medicine and National Research Council,

2005; Tabar et al., 2011; Canadian Task Force on Preventive Health Care, 2011; Marmot et al., 2013).

Furthermore, patients with suspected breast cancer need to have a biopsy which is frequently used to con- firm the diagnosis before treatment is planned (Millis,1984).

Generally, a biopsy is conducted by taking a sample of tissue from a suspicious area. Next, the sample is stained with hematoxylin and eosin (H&E) substance used to differentiate a nucleus with a parenchyma. The difference can be observed through an optical microscope; moreover, the images seen through the microscope are captured as giga-pixel images and commonly named as whole-slide images (WSI) for further digital image processing, such as cancer cell segmentation or detection (Aresta et al., 2019).

---

[a] https://orcid.org/0000-0002-5150-4394
[b] https://orcid.org/0000-0003-0586-8880
[c] https://orcid.org/0000-0001-6198-7484
[d] https://orcid.org/0000-0002-0800-9937

Biopsy diagnosis from histopathological images is considered a gold standard for determining almost all types of cancer, specifically BC International Agency for Research on Cancer, 2012; David
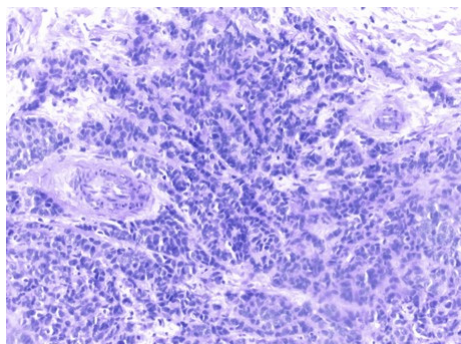

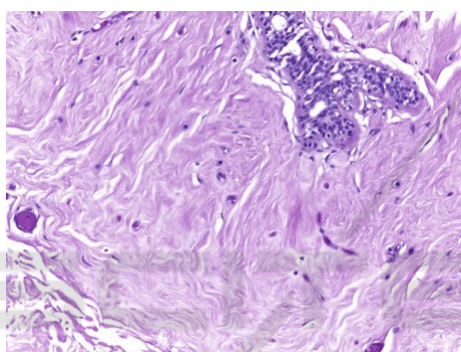Figure 1: An image of malignant cells.
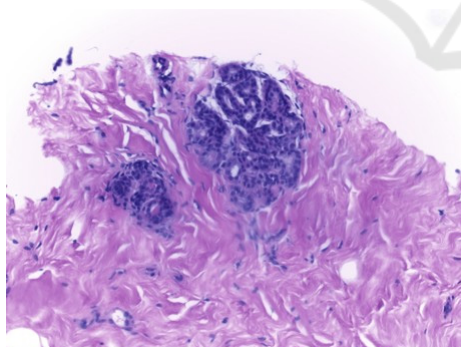

Figure 2: An image of benign cells.

Figure 3: An image of normal cells.

S. Strayer, 2014). Properties of the histo-pathological images are analyzed by pathologists in order to find types of the breast cancers. Figure 1 and Figure 2 show malignant and benign cancer cells while Figure 3 shows normal cells.

In developing countries, such as Indonesia, the ratio of physician to population is still lower than the WHO-recommended figure; moreover, ongoing geo-graphical disparities exist which exacerbate the short-

age of physicians (Asia Pacific Observatory on Health Systems and Policies, 2017). With the advent of Artificial Intelligence (AI), particularly deep learning, there are vast opportunities to help classify types of BC with some degrees of automation.

are datasets which charge the deep learning algorithms. Fortunately, international research organizations such as Pathological Anatomy and Cytopathology (P&D) Laboratorium in Parana, Brazil Spanhol et al., 2016), the Institute of Molecular Pathology and Immunology of the University of Porto (IPATIMUP) and the Institute for Research and Innovation in Health (i3S) in Porto, Portugal (Aresta et al., 2019), and Center for Bio-Image Informatics, University of California in Santa Barbara, USA (Gelasca et al., 2008) have released publicly available BC histopathological image datasets.

Each publicly available dataset has its own characteristic; furthermore, combining these characteristics into a unified dataset will make a rich learning dataset for deep learning models. A deep learning model which learns from the unified dataset will be better in generalization on unseen data than the one learns from only one dataset (Geron, 2019). Therefore, firstly this paper also provides a unified dataset as a new publicly available dataset to help this research field progress.

Secondly, the paper initializes a deep learning model which functions as a baseline on the new unified dataset. After the Vahadane preprocessing technique (Vahadane et al., 2016) is applied into our unified dataset, we feed the preprocessed dataset into a model which employs a progressive resizing approach (Howard and Gugger, 2020). Both the preprocessing technique and the resizing approach are suitable to our problem; hence, the performance of our model has soared and put the model among state-of-the-art models for BC histopathological image classification problem.

In the remainder of this paper, we first explore related work which delves into various datasets and relevant BC histopathological image classification techniques. Next, we turn our attention to the Vahadane preprocessing technique and progressive resizing. Finally, we discuss our results and conclude with a few general observations and directions for future work

2 RELATED WORK

The related work of our paper discusses BC histopathological images datasets and relevant BC classification techniques.

2.1 Histopathological Image Datasets

We have searched and found three publicly accessible datasets on the Internet that are BreaKHis (Spanhol et al., 2016), BACH (Aresta et al., 2019), and UCSB benchmark dataset for bioimaging application (Gelasca et al., 2008).

The BreaKHis consists of 7,909 BC histopathological images taken from 82 patients from January 2014 to December 2014 with different magnifying factors (40, 100, 200, and 400) (Spanhol et al., 2016). Moreover, the numbers of benign and malignant cases are 2,480 and 5,429 respectively. The benign category includes adenosis (A), fibroadenoma (F), phyllodes tumor (PT), and tubular adenoma (TA); additionally, the malignant category covers ductal carcinoma (DC), lobular carcinoma (LC), mucinous carcinoma (MC), and papillary carcinoma (PC). Laboratorium P&D (Pathological Anatomy and Cytopathology, Parana, Brazil) has published this dataset for research purposes.

The BACH was released as a grand challenge on BC histopathological images which is a part of the 15th International Conference on Image Analysis and Recognition (ICIAR 2018). The annotation for the dataset was done by pathologists from the Institute of Molecular Pathology and Immunology of the University of Porto (IPATIMUP) and the Institute for Research and Innovation in Health (i3S) (Aresta et al., 2019). The histopathological images were obtained from patients in Porto and Castelo Branco area, Portugal in year 2014, 2015, and 2017. The dataset consists of microscopy dataset and whole-slide images dataset; specifically, the whole-side images dataset is used for an image segmentation task besides. Ourresearch employs the microscopy dataset which categorizes BC cells into 1) benign, 2) malignant, 3) in situ carcinoma, and 4) invasive carcinoma. Furthermore, the dataset is composed of 400 training imagesand 100 test images with equal number of images in each category.

The third dataset is University of California, Santa Barbara (UCSB) benchmark dataset for bioimaging application (Gelasca et al., 2008). The dataset comprises of 58 histopathological images which are used for BC histopathological image classification taskwith associated ground truth data available.

2.2 Histopathological Classification Techniques

Prior work has established several techniques to solve BC histopathological images classification problem. An early BC histopathological classification technique begins with three extracted features from images, that are curvelet transform, statistical data from Gray Level Co-occurrence Matrix (GLCM), and Completed Local Binary Patterns (CLBP) (Zhanget al., 2011). Next, these three features construct an input layer for Random Subspace Ensemble (Skurichina and Duin, 2002).

The Random Subspace Ensemble in their research comprises 20 multi-layer perceptron (MLP) whose number of hidden layers are random values in range between 30 and 50 inclusively. The accuracy of the model has achieved 95.22% on the 3-class (normal, in situ carcinoma, and invasive carcinoma) dataset released by the ComputerScience department of Israel Institute of Technologywhich is, unfortunately, not publicly available.

Other prior work employs a combination of Convolutional Neural Network (CNN) and a Support Vector Machines classifier on BACH dataset (Araujo et al., 2017). This combination model achieves accuracies of 77.8% for four-class and 83.3% for carcinoma/non-carcinoma BC classification tasks and recall of 95.6%. Another work on BACH dataset comes from combining several deep neural networks and gradient boosted trees classifiers (Rakhlin et al., 2018). The model gains 87.2% accuracy and 93.8% accuracy for 4-class classification and 2-class classification task respectively. Lastly, a work on BACHdataset fine-tunes Inception-v3 CNN with a strategyfor image patches extraction (Golatkar et al., 2018).The Inception-v3 model acquires accuracy of 85% over four classes and 93% for non-cancer (normal orbenign) vs. malignant (in situ or invasive carcinoma). A current state-of-the-art technique, which outperforms the previous work by Araujo et al. (2017), Rakhlin et al. (2018), and Golatkar et al. (2018) forms a new hybrid convolutional and recurrent deep neural network enriched with multilevel feature representation of image patches (Yan et al., 2020). This technique combines the strengths of convolutional and recurrent neural networks and preserves the short-term and long-term spatial correlations among thepatches. The method achieves an average accuracy of 91.3% for 4-class classification task. Unfortunately, the dataset of this work is not available for outside of China.

3 RESEARCH METHODOLOGY

Our research methodology consists of merging the dataset, preprocessing the dataset, building the baseline, and constructing progressive resizing approach.

3.1 Merging the Dataset

Three different datasets (Spanhol et al., 2016; Aresta et al., 2019; Gelasca et al., 2008) have different classes; therefore, in order to merge those different classes, those labels need adjusting. Firstly, the classes in BreaKHis dataset are benign and malig- nant. The benign class has subclasses: adenosis, fi- broadenoma, phyllodes tumor, and tubular adenoma, while the malignant class consists of adenosis, fi- broadenoma, phyllodes tumor, and tubular adenoma. Secondly, BACH dataset have four classes, such as normal, benign, in situ carcinoma, and invasive carci- noma. Lastly, UCSB benchmark dataset has benign and malignant classes. After considering the number of classes, we opt to choose three classes, that are normal, benign, and malignant. Specifically, both in situ carcinoma and invasive carcinoma of the BACH are joined into the malignant class of the new unified dataset.

3.2 Color Normalization

Next, the Vahadane technique which combines Sparse Non-negative Matrix Factorization (SNMF) and Structure-preserving Color Normalization (SPCN) (Vahadane et al., 2016) is applied into our images. Particularly, the Vahadane technique solves both stain separation and color normalization problems. The stain separation problem is cast into a non-negative matrix factorization (NMF) with an addition of a sparseness constraint. Moreover, the color basis of an image is substituted by the one of a pathologist-preferred target image. This is the algorithm of SPCN whose advantage is to maintain the image's original stain concentrations. The way SPCN works is through replacing the color basis of a source image with those of a pathologist-preferred target image, while still maintaining its original stain concentrations. The flexibility to select a preferred target appearance in different scenarios as opposed to a fixed target color appearance model is another advantage of our technique over others such as Macenko et al. (2009).

3.3 Building the Baseline

ResNet-34 (He et al., 2016) is chosen to be the baseline for our experiment because ResNet architecture which relies on residual connections is the most widely used architecture and proven to be a strong baseline among CNN architectures; furthermore, recent development in image classification models is getting more and more on using the same trick of residual connections or tweaking the original ResNet architecture (Howard and Gugger, 2020).

3.4 Constructing Progressive Resizing Approach

Progressive resizing approach was one of the most important innovations when fast.ai and its team won the DAWNBench Competition in 2018 (Howard and Gugger, 2020). The idea is very simple, that is to start training using small images and finally end the training using large images. Training with small images for most of the epochs helps finishing the training much faster. Additionally, completing training with large images achieves a much higher final accuracy. Progressive resizing is also another strategy of data augmentation. Accordingly, better generalization of our models should be expected when they are trained with progressive resizing.

4 RESULTS

4.1 The Unified Dataset

The unified dataset has three classes such as normal, benign, and malignant.

Table 1: Statistics of image sizes which consist of mean, standard deviation, minimum, Q1, Q2, Q3, and maximum (measurement unit: pixel).

Statistics	Width	Height
Count	$8,367.000$	$8,367.000$
Mean	513.540	765.802
Standard deviation	230.537	287.778
Minimum	456.000	700.000
Q_1	460.000	700.000
Q_2 (median)	460.000	700.000
Q_3	460.000	700.000
Maximum	$1,536.000$	$2,048.000$

Table 1 shows the statistics of our unified dataset. Furthermore, 70% of the dataset is chosen randomly to be training set and the rest is determined as validation set. The code to unify the three datasets can be viewed in the github repository.

4.2 Normalizing Colors of Images

We employ StainTools library to do the normalization. The library can be found at Peter Byfield's github repository[e].
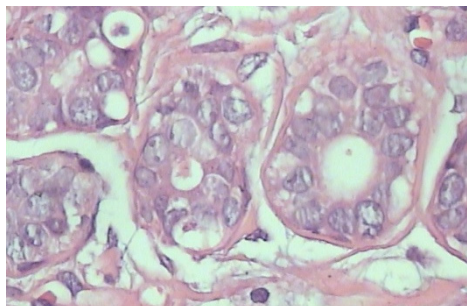

Figure 4: An image before applying Vahadane normalization.

Figure 4 and Figure 5 show an example of an image before and after normalization respectively. Briefly, normalization is a process of replacing the color basis of a source image with those of a pathologist-preferred target image, while still maintaining its original stain concentrations.
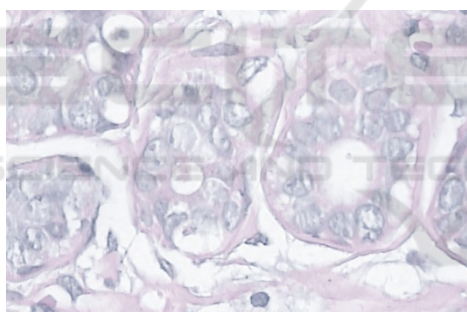

Figure 5: An image after applying Vahadane normalization.

4.3 Performance of the First Baseline

ResNet-34 model as a baseline is created by employing fast.ai library. Before the model is trained with the unified dataset, all images are resized into the mean of width and height of the images that is 514 pixels by 766 pixels respectively; specifically, the resizing technique does not preserve the aspect ratio of the images. In addition, the standard of one epoch is used to do a fine-tuning process on the pre-trained ResNet-34 (Howard and Gugger, 2020).

Table 2: The F_1 scores of the the baseline by fine-tuning ResNet-34 pre-trained model (Train = train loss, Valid = validation loss; the higher the F_1 score is, the better the performance of the baseline is).

Epoch	Train	Valid	F_1 score	Time
0	0.636	0.516	85.547%	19:06
Epoch	Train	Valid	F_1 score	Time
0	0.104	0.741	**83.733%**	05:13

Table 2 displays the performance of ResNet-34 model. We opt to use F_1 score as our performance metric since the number of instances in each class of our dataset are imbalanced and F_1 is the best choice for measuring performance on imbalanced datasets (Sokolova and Lapalme, 2009).

4.4 Performance of the Progressive Resizing

To assess the effect of progressive resizing, we construct another baseline (ResNet-50) based on a data augmentation technique, the so-called presizing trick. Firstly, we resize all images to dimensions that are significantly larger than the target training dimensions. Next, we arrange all common augmentation operations including a resize to the final target size into one big chuck of operation, and finally performing the operation on the GPU only once at the end oftrick.
The ResNet-50 enhanced with a presizing trick is quite a strong baseline (F_1 score of 98.443%). However, we can still improve the performance of the model by using the progressive resizing. Firstly, we normalize our input data (Z-normalization) so it has a mean of 0 and a standard deviation of 1 and verify the effect of Z-normalization on training the model.

Table 3: The F_1 scores of the the second baseline (ResNet-50) by using presizing trick (Train = train loss, Valid = validation loss; the higher the F_1 score is, the better the performance of the baseline is).

Epoch	Train	Valid	F_1 score	Time
0	0.313	0.312	91.196%	03:40
1	0.213	0.808	74.228%	03:39
2	0.160	0.089	97.547%	03:38
3	0.116	0.048	97.976%	03:38
4	0.079	**0.0315**	**98.443%**	03:38

---

[e] https://github.com/Peter554/StainTools

Table 4: F_1 scores of the the third baseline (ResNet-50) by using presizing trick and Z-normalization (Train = train loss, Valid = validation loss; the higher the F_1 score is, the better the performance of the baseline is).

Epoch	Train	Valid	F_1 score	Time
0	0.578	0.376	93.182%	03:40
1	0.239	0.249	93.90%	03:40
2	0.148	0.046	98.384%	03:38
3	0.092	0.038	98.626%	03:39
4	0.072	**0.037**	**98.682%**	03:38

Table 4 shows utilizing *Z*-normalization improves F_1 score a little; however, *Z*-normalization on input data becomes a standard when working with pre-trained models. Next, we employ the progressive resizing approach by starting a training with small images (128 pixels by 128 pixels) and ending the training using large images (the original image size). This approach works because features learned by early layers of CNNs are not quite specific to the size of an image as the layers find curves and edges. Moreover, thesubsequent layers may later find shapes such as cell shapes. Therefore, changing image size in the middle of the training does not mean that the parameters of the models are completely different; it just requiresthe models to learn a little bit differently, that is by using transfer learning, in other words, fine-tuning.

Table 5: F_1 scores of finding an optimal learning rate by Cyclical Learning Rates method (Train = train loss, Valid = validation loss; the higher the F_1 score is, the better the performance of the baseline is).

Epoch	Train	Valid	F_1 score	Time
0	0.931	0.963	78.857%	03:21
1	0.397	0.109	95.593%	03:22
2	0.198	0.053	97.787%	03:21
3	0.115	0.042	98.426%	03:20

Table 5 displays the process of finding an optimal learning rate by Cyclical Learning Rates (Smith, 2017).

Table 6: F_1 scores of fine-tuning ResNet-50 as a part of progressive resizing approach (Train = train loss, Valid = validation loss; the higher the F_1 score is, the better the performance of the baseline is).

Epoch	Train	Valid	F_1 score	Time
0	0.109	0.049	97.117%	03:39
Epoch	Train	Valid	F_1 score	Time
0	0.081	0.044	98.501%	03:40
1	0.097	0.033	98.861%	03:39
2	0.076	0.025	98.981%	03:38
3	0.060	0.025	98.924%	03:39
4	0.050	0.022	**99.102%**	03:38

Table 6 shows that utilizing progressive resizing approach achieves F_1 score of 99.102%. Although our performance cannot be compared to the current state-of-the-art (Yan et al., 2020) and other previous works because of different metrics (Araujo et al., 2017; Rakhlin et al., 2018; Golatkar et al., 2018) and dataset (Yan et al., 2020), to the best of our knowledge, the performance of our approach is among the highest BC classification model considering its nearlyperfect F_1 score. Source codes of our approach are publicly available at our github repository.

5 CONCLUSIONS

We have created a unified dataset merged from three popular datasets and propose the dataset for advancing research in BC classification field. Moreover, in addition to the dataset contribution, we also provided a strong model using progressive resizing approach whose F_1 score is 99.102%. We argue that our model is comparable among other state-of-the-art models for the dataset.

REFERENCES

Araujo, T., Aresta, G., Castro, E., Rouco, J., Aguiar, P., Eloy, C., Polonia, A., and Campilho, A. (2017). "Classification of Breast Cancer Histology Images using Convolutional Neural Networks". PLOS ONE, 12(6), 1-14.

Aresta, G., Araujo, T., Kwok, S., Chennamsetty, S. S., Safwan, M., Alex, V., Marami, B., Prastawa, M., Chan, M., Donovan, M., et al. (2019). "BACH: Grand Challenge on Breast Cancer Histology Images". *Med. Image Anal.* 6(1), 122-139.

Asia Pacific Observatory on Health Systems and Policies (2017). "The Republic of Indonesia Health System

Review. *Health Systems Tran.* 7(1), 24-30.

Bray, F., Ferlay, J., Soerjomataram, I., Siegel, R. L., Torre, L. A., and Jemal, A. (2018). " Global Cancer Statistics 2018: Globocan Estimates of Incidence and Mortality Worldwide for 36 Cancers in 185 Countries". *CA: A Cancer J. Clin.* 68(6), 394-424.

Canadian Task Force on Preventive Health Care (2011). "Recommendations on Screening for Breast Cancer in Average-risk Women Aged 40-74 Years". *Cmaj*, 183(17), 1991-2001.

David S. Strayer, E. R. (2014). *Rubin's Pathology: Clinico-pathologic Foundations of Medicine (Pathology (Rubin)) Seventh Edition*. LWW.

Gelasca, E. D., Byun, J., Obara, B., and Manjunath, B. (2008). "Evaluation and Benchmark for Biological Image Segmentation". In *2008 15th IEEE International Conference on Image Processing*, 1816-1819. IEEE.

Geron, A. (2019). *Hands-on Machine Learning with Scikit-Learn, Keras, and TensorFlow: Concepts, Tools, and Techniques to Build Intelligent Systems Second Edition*. O'Reilly Media Inc.

Golatkar, A., Anand, D., and Sethi, A. (2018). "Classification of Breast Cancer Histology using Deep Learning". In *International Conference Image Analysis and Recognition*, 837-844. Springer.

He, K., Zhang, X., Ren, S., and Sun, J. (2016). "Deep Residual Learning for Image Recognition". In *Proceedings of the IEEE Conference on Computer Vision and Pattern Recognition*, 770-778.

Howard, J. and Gugger, S. (2020). *Deep Learning for Coders with fastai and PyTorch*. O'Reilly Media Inc.

Institute of Medicine and National Research Council (2005). *Saving Women's Lives: Strategies for Improving Breast Cancer Detection and Diagnosis*. The National Academies Press, Washington, DC.

International Agency for Research on Cancer (2012). *WHO Classification of Tumours of the Breast [OP] (Medicine) 4th Edition*. World Health Organization.

Macenko, M., Niethammer, M., Marron, J. S., Borland, D., Woosley, J. T., Guan, X., Schmitt, C., and Thomas, N. E. (2009). "A Method for Normalizing Histology Slides for Quantitative Analysis". In 2009 IEEE International Symposium on Biomedical Imaging: From Nano to Macro, 1107-1110. IEEE.

Marmot, M. G., Altman, D., Cameron, D., Dewar, J., Thompson, S., and Wilcox, M. (2013). "The Benefits and Harms of Breast Cancer Screening: An Independent Review". *British Journal of Cancer*, 108(11), 2205.

McKinney, S. M., Sieniek, M., Godbole, V., Godwin, J., Antropova, N., Ashrafian, H., Back, T., Chesus, M., Corrado, G. C., Darzi, A., Etemadi, M., Garcia-Vicente, F., Gilbert, F. J., Halling-Brown, M., Hassabis, D., Jansen, S., Karthikesalingam, A., Kelly, C. J., King, D., Ledsam, J. R., Melnick, D., Mostofi, H., Peng, L., Reicher, J. J., Romera-Paredes, B., Sidebottom, R., Suleyman, M., Tse, D., Young, K. C., De Fauw, J., and Shetty, S. (2020). "International Evaluation of an AI System for Breast Cancer Screening". *Nat.* 577(7788), 89-94.

Millis, R. R. (1984). "Needle Biopsy of the Breast". *Monog. Pathol.* (25), 186-203.

Rakhlin, A., Shvets, A., Iglovikov, V., and Kalinin, A. A. (2018). "Deep Convolutional Neural Networks for Breast Cancer Histology Image Analysis". In *International Conference Image Analysis and Recognition*, 737-744. Springer.

Skurichina, M. and Duin, R. P. (2002). " Bagging, Boosting and the Random Subspace Method for Linear Classifiers". *Pattern Anal. Appl.* 5(2), 121-135.

Smith, L. N. (2017). "Cyclical Learning Rates for Training Neural Networks". In 2017 *IEEE Winter Conference on Applications of Computer Vision* (WACV), 464-472. IEEE.

Sokolova, M. and Lapalme, G. (2009). "A Systematic Analysis of Performance Measures for Classification Tasks". *Infor. Proc. Manage.* 45(4), 427-437.

Spanhol, F. A., Oliveira, L. S., Petitjean, C., and Heutte, L. (2016). "A Dataset for Breast Cancer Histopathological Image Classification". *IEEE Trans. on Biomedical Engineering*, 63(7), 1455-1462.

Stenkvist, B., Westman-Naeser, S., Holmquist, J., Nordin, B., Bengtsson, E., Vegelius, J., Eriksson, O., and Fox, C. H. (1978). "Computerized Nuclear Morphometry as an Objective Method for Characterizing Human Cancer Cell Populations". *Cancer Res.* 38(12), 4688-4697.

Tabar, L., Vitak, B., Chen, T. H.-H., Yen, A. M.-F., Cohen, A., Tot, T., Chiu, S. Y.-H., Chen, S. L.-S., Fann, J. C. Y., Rosell, J., et al. (2011). "Swedish Two-county Trial: Impact of Mammographic Screening on Breast Cancer Mortality during 3 Decades". Radiology, 260(3), 658-663.

Vahadane, A., Peng, T., Sethi, A., Albarqouni, S., Wang, L., Baust, M., Steiger, K., Schlitter, A. M., Esposito, I., and Navab, N. (2016). "Structure-preserving Color Normalization and Sparse Stain Separation for Histological Images. *IEEE Transactions on Medical Imaging*, 35(8), 1962-1971.

World Health Organization (2018). Data Global Can- cer Observatory 2018. https://gco.iarc.fr/today/data/factsheets/populations/360-indonesia-fact-sheets.pdf. Accessed: 2020-01-04.

Yan, R., Ren, F., Wang, Z., Wang, L., Zhang, T., Liu, Y., Rao, X., Zheng, C., and Zhang, F. (2020). Breast Cancer Histopathological Image Classification using a Hybrid Deep Neural Network. *Meth.* 173(1), 52-60.

Zhang, Y., Zhang, B., and Lu, W. (2011). Breast Cancer Classification from Histological Images with Multiple Features and Random Subspace Classifier Ensemble. In *AIP Conference Proceedings*, 1371(1), 19-28.